"eliminated" molecule in the fifth position of the trigonal-bipyramid (η^2-H_2 complex).

Finally, we have compared and contrasted the reactivities of a series of isoelectronic metal fragments, namely $[(NP_3)M]^+$ and $[(PP_3)M]^+$ (M = Co, Rh, Ir), toward aromatic C-H bond activation. It appears that for those systems for which C-H oxidative addition is thermodynamically allowed (Rh, Ir), steric crowding favors the intramolecular ortho-metalation reaction.

Acknowledgment. We are grateful to Prof. A. Vacca for helpful discussion and to P. Innocenti and A. Traversi for technical assistance.

Registry No. 1, 85233-90-5; **2**, 110827-50-4; **3**, 115590-80-2; **4**, 115590-82-4; **5**, 80602-44-4; **6**, 115590-83-5; **7**, 85233-91-6; **8**, 109786-30-3; **9c**, 115590-84-6; **10**, 115590-86-8; **11**, 110827-48-0; **12**, 110827-49-1; **13**, 110827-46-8; **14**, 110827-47-9; **15**, 104910-92-1; **16**, 115591-02-1; **17**, 115590-88-0; **17a**, 115591-00-9; **18**, 114900-45-7; **19**, 114900-46-8; **20**, 89530-44-9; **21**, 115590-90-4; **22**, 114900-38-8; **23**, 115590-92-6; **24** (isomer 1), 109786-34-7; **24** (isomer 2), 109837-84-5; **25**, 115590-94-8; **26**, 115590-95-9; **27**, 115590-97-1; **28**, 115590-99-3; **29**, 95911-60-7; I, 15114-55-3; II, 23582-03-8; NP_3Cy, 115562-61-3; $[RhCl(COD)]_2$, 12092-47-6; $[(NP_3)RhCl_2]BPh_4$, 85233-87-0.

Supplementary Material Available: Refined anisotropic and isotropic temperature factors (Table VII) and final positional parameters for hydrogen atoms for **17a** (Table VIII) (5 pages); listing of observed and calculated structure factors for **17a** (42 pages). Ordering information is given on any current masthead page.

Reactivity of Trimethylaluminum with $(C_5Me_5)_2Sm(THF)_2$: Synthesis, Structure, and Reactivity of the Samarium Methyl Complexes $(C_5Me_5)_2Sm[(\mu\text{-}Me)AlMe_2(\mu\text{-}Me)]_2Sm(C_5Me_5)_2$ and $(C_5Me_5)_2SmMe(THF)$[1]

William J. Evans,* L. R. Chamberlain, Tamara A. Ulibarri, and Joseph W. Ziller

Contribution from the Department of Chemistry, University of California, Irvine, Irvine, California 92717. *Received November 12, 1987*

Abstract: $(C_5Me_5)_2Sm(THF)_2$ reduces $AlMe_3$ in toluene to form $(C_5Me_5)_2Sm[(\mu\text{-}Me)AlMe_2(\mu\text{-}Me)]_2Sm(C_5Me_5)_2$ (**1**), which crystallizes from toluene in space group $P2_1/n$ with unit cell parameters a = 12.267 (3) Å, b = 12.575 (3) Å, and c = 17.131 (2) Å and z = 2 for D_{calcd} = 1.30 g cm^{-3}. Least-squares refinement of the model based on 2163 observed reflections converged to a final R_F = 5.7%. Each trivalent bent metallocene $(C_5Me_5)_2Sm$ unit in **1** is connected to two tetrahedral $(\mu\text{-}Me)_2AlMe_2$ moieties via nearly linear Sm(μ-Me)-Al linkages (175.2 (9)° and 177.8 (7)° angles). The average Sm-C(μ-Me) distance is 2.75 (2) Å. In solution, **1** is in equilibrium with the monomer $(C_5Me_5)_2Sm(\mu\text{-}Me)_2AlMe_2$. THF cleaves the bridging $AlMe_4$ units in **1** liberating $AlMe_3$ and $(C_5Me_5)_2SmMe(THF)$ (**2**). **2** crystallizes from THF/hexane in space group *Pnma* with unit cell parameters a = 18.0630 (42) Å, b = 15.6486 (39) Å, and c = 8.7678 (15) Å and Z = 4 for D_{calcd} = 1.36 g cm^{-3}. Least-squares refinement of the model based on 2087 observed reflections converged to a final R_F = 7.0%. The bent metallocene $(C_5Me_5)_2Sm$ unit is coordinated to the methyl group and to THF with Sm-C and Sm-O distances of 2.484 (14) and 2.473 (9) Å, respectively. **2** reacts with aromatic and aliphatic hydrocarbons including benzene, toluene, hexane, cyclohexane, and cyclooctane liberating CH_4 via net activation of C-H bonds. The benzene and toluene reactions form $(C_5Me_5)_2Sm(C_6H_5)(THF)$ and $(C_5Me_5)_2Sm(CH_2C_6H_5)(THF)$, respectively, in high yield. The other reactions form complex mixtures of organosamarium products. The methane generated in the reactions of **2** with deuteriated substrates is CH_4, which suggests that intramolecular formation of a spectroscopically undetected intermediate containing a metalated C_5Me_5 ring may occur before intermolecular reaction with the C-H bond. The benzene reaction has a moderate enthalpy of activation (16.5 ± 0.6 kcal/mol) and a large negative entropy of activation (−19 ± 4 eu), consistent with the "σ-bond metathesis" mechanism proposed for C-H bond activation at electron-deficient metal centers. **2** metalates pyridine-d_5 to form CH_3D, reacts with Et_2O to form $(C_5Me_5)_2Sm(OEt)(THF)$, and reacts with H_2 to form $[(C_5Me_5)_2Sm(\mu\text{-}H)]_2$. Both **1** and **2** polymerize ethylene.

The low-valent organolanthanide complex $(C_5Me_5)_2Sm(THF)_2$[2-4] has recently been shown to effect remarkable transformations of unsaturated organic substrates including CO,[5] RC≡CR,[6] RCH=CHR,[7] and RN=NR.[8] Much of the reactivity observed was unprecedented, which suggested that the full potential of $(C_5Me_5)_2Sm(THF)_2$ could best be defined by exploratory studies with a range of substrates. To expand our knowledge of the reactivity of $(C_5Me_5)_2Sm(THF)_2$, we have begun to explore reactions with organometallic and inorganic substrates. In this report, we describe the reaction of $(C_5Me_5)_2Sm(THF)_2$ with trimethylaluminum. This system provides an unusual tetrametallic $AlMe_4^-$ bridged complex and, in addition, an excellent synthetic route to the first compound containing a terminal methyl group attached to a samarium ion.[9] Both complexes function

(1) Reported in part at the 2nd International Conference on the Basic and Applied Chemistry of f-Transition (Lanthanide and Actinide) and Related Elements, Lisbon, Portugal, April 1987, L(II)1, and at the 193rd National Meeting of the American Chemical Society, Denver, CO, April 1987, INOR 227.

(2) Evans, W. J.; Grate, J. W.; Choi, H. W.; Bloom, I.; Hunter, W. E.; Atwood, J. L. *J. Am. Chem. Soc.* **1985**, *107*, 941-946.

(3) Evans, W. J. In *High-Energy Processes in Organometallic Chemistry*; K. S. Suslick, Ed.; American Chemical Society: Washington, DC, 1987; ACS Symp. Ser. No. 333, pp 278-289.

(4) Evans, W. J. *Polyhedron* **1987**, *6*, 803-835.

(5) Evans, W. J.; Grate, J. W.; Hughes, L. A.; Zhang, H.; Atwood, J. L. *J. Am. Chem. Soc.* **1985**, *107*, 3728-3730.

(6) Evans, W. J.; Hughes, L. A.; Drummond, D. K.; Zhang, H.; Atwood, J. L. *J. Am. Chem. Soc.* **1986**, *108*, 1722-1723.

(7) Evans, W. J.; Drummond, D. K. *J. Am. Chem. Soc.* **1988**, *110*, 2772-2774.

(8) Evans, W. J.; Drummond, D. K. *J. Am. Chem. Soc.* **1986**, *108*, 7440-7441.

(9) The bridging methyl samarium complex $Sm(\mu\text{-}Me)_6Li_3(Me_2NCH_2CH_2NMe_2)_3$ is known: Schumann, H.; Muller, J.; Bruncks, N.; Lauke, H.; Pickardt, J.; Schwarz, H.; Eckart, K. *Organometallics* **1984**, *3*, 69-74.

0002-7863/88/1510-6423$01.50/0

as polymerization catalysts, and the latter compound is highly reactive in C–H activation reactions.[10-19] The synthesis, structure, and reactivity of these compounds are described in this report.

Experimental Section

All compounds described below are extremely air- and moisture-sensitive. Therefore, all syntheses and subsequent manipulations involving these materials were conducted under nitrogen with the rigorous exclusion of air and water with the use of Schlenk, high-vacuum, and glovebox (Vacuum/Atmospheres HE-553 Dri-Lab) techniques.

Materials. Tetrahydrofuran (THF), diethyl ether, pyridine, toluene, hexane, cyclohexane, and cyclooctane were distilled or vacuum transferred from solutions of sodium benzophenone ketyl. THF-d_8, benzene-d_6, cyclohexane-d_{12}, and pyridine-d_5 were vacuum transferred from sodium benzophenone ketyl. Ethylene (Matheson) was used as received. $(C_5Me_5)_2Sm(THF)_2$ was prepared from $SmI_2(THF)_2$ and KC_5Me_5 as previously described.[2]

Physical Measurements. ^1H and ^{13}C NMR spectra were obtained on GE 300-MHz and GN 500-MHz NMR spectrometers. DEPT experiments[20] were performed on the GN 500-MHz NMR. Chemical shifts were assigned relative to C_6D_5H, 7.15 ppm, for spectra in benzene-d_6, relative to proteocyclohexane, 1.40 ppm, for spectra in cyclohexane-d_{12}, relative to proteopyridine, 8.80 ppm, for spectra in pyridine-d_5, or relative to proteo-THF, 1.79 ppm, for spectra in THF-d_8. Infrared spectra were measured as KBr pellets and recorded by using a Perkin-Elmer 283 infrared spectrometer. Magnetic moments were obtained on a Bruker 250-MHz NMR spectrometer by the Evans method.[21] Gas evolution measurements were performed by using standard Toepler techniques and the gases were identified by mass spectrometry. Mass spectra were recorded by using a Finnegan 4000 mass spectrometer. Complete elemental analyses were obtained from Analytische Laboratorien, Engelskirchen, West Germany. Polyethylene molecular weights were obtained by gel permeation chromatography in trichlorobenzene at the Unocal Science and Technology Division, Brea, CA.

$(C_5Me_5)_2Sm[(\mu\text{-Me})AlMe_2(\mu\text{-Me})]_2Sm(C_5Me_5)_2$ (1). In the glovebox, excess $AlMe_3$ (1.0 mL, 10.4 mmol) was added at ambient temperature to a purple solution of $(C_5Me_5)_2Sm(THF)_2$ (100 mg, 0.176 mmol) in 15 mL of toluene. The reaction was stirred and turned dark brown within 5 min. After standing 24 h, the reaction solution was red-orange and a blackish, metallic-like precipitate had formed. The reaction was filtered and the precipitate was washed with hot toluene. The filtrates were combined and the solvent was removed by rotary evaporation. The resulting orange solid was dissolved in hot toluene and slowly cooled to −34 °C to yield **1** as red-orange crystals (97 mg, 80%). Anal. Calcd for $C_{24}H_{42}SmAl$: C, 56.75; H, 8.33; Sm, 29.61; Al, 5.31. Found: C, 55.19; H, 7.50; Sm, 31.10; Al, 5.92. Magnetic susceptibility: $\chi_M^{293K} = 1085 \times 10^{-6}$ cgs; $\mu_{eff}^{293K} = 1.6\ \mu_B$. ^1H NMR (C_6D_6, 25 °C [$\Delta\nu_{1/2}$ in Hz]): **1a**, 0.87 [23] (s, C_5Me_5), −2.26 [35] (s, $(\mu\text{-}Me)_2Al\mathit{Me}_2$), −14.3 [60] (s, $(\mu\text{-}\mathit{Me})_2AlMe_2$); **1b**, 0.69 [7] (s, $C_5\mathit{Me}_5$), 1.63 [16] (s, $(\mu\text{-Me})_2Al\mathit{Me}_2$), −17.6 [44] (s, $(\mu\text{-}\mathit{Me})_2AlMe_2$). ^{13}C NMR ($CD_3C_6D_5$, 20° C): **1a**, 119.2, C_5Me_5; 19.8, $C_5\mathit{Me}_5$; **1b**, 118.4, C_5Me_5; 18.9, $C_5\mathit{Me}_5$. IR (KBr) 2900 s, 1438 m, 1375 m, 1180 m, 1015 w, 927 s, 735 m, 672 w, 615 w cm^{-1}.

The synthesis of **1** was also conducted in a vacuum system attached to a Toepler pump in order to monitor gases evolved during the synthesis. $(C_5Me_5)_2Sm(THF)_2$ (309 mg, 1.09 mmol) in 15 mL of toluene was placed in a tube fitted with a high-vacuum greaseless stopcock, a 24/40 joint, and a sidearm capped with a septum. The tube was connected to a vacuum line and 5 freeze–pump–thaw cycles were carried out on the solution. After the tube warmed to room temperature, $AlMe_3$ (0.89 mL, 9.3 mmol) was injected into the reaction vessel. In 12 h the color changed from purple to red-orange and a finely divided black powder precipitated from solution. The gas evolved during the reaction was collected via a Toepler pump and was found to be methane by mass spectrometry (16.74 mL, 0.04 mmol). The reaction solution was taken into the glovebox and the solution was decanted. The black precipitate which adhered to the reaction vessel was quickly washed with hexane and the tube was reattached to the vacuum line. Approximately 10 mL of D_2O was then vacuum transferred into the tube. There was no immediate bubbling from the surface. However, after 10 h, the surface was vigorously reacting with the D_2O. The gases evolved were collected via a Toepler pump and were found to be D_2 and methane by mass spectrometry.

To study the solution equilibrium between the monomeric and dimeric forms of **1**, a freshly prepared sample of **1** (15 mg, 0.015 mmol) was sealed in an NMR tube in 0.45 mL of toluene-d_8 (0.033 M solution). Nine ^1H NMR spectra were obtained between the temperatures of −25 and 55 °C at 10-deg intervals. After each temperature change, 15 min were allowed for the sample to equilibrate. The equilibrium constants at each temperature were calculated as follows: K_{obsd} = [monomer]^2/[dimer]. At a given temperature the concentration of each individual species was determined by monitoring the relative intensities of the C_5Me_5 peaks using the peak of residual proteotoluene in toluene-d_8 as an internal integration standard. ΔH and ΔS values were determined from the slope and intercept of the line generated by plotting ln K_{obsd} versus $1/T$.

X-ray Data Collection, Structure Determination, and Refinement for 1. A red-orange crystal of approximate dimensions 0.12 × 0.17 × 0.26 mm was mounted in a thin-walled glass capillary under nitrogen and accurately aligned on a Syntex $P2_1$ diffractometer. Subsequent setup operations (determination of accurate unit cell dimensions and orientation matrix) and collection of room temperature (22 °C) intensity data were carried out with standard techniques.[22] Details are given in Table I.

The systematic extinctions $h0l$ for $h + l = 2n + 1$ and $0k0$ for $k = 2n + 1$ uniquely identified the space group as $P2_1/n$, a nonstandard setting of the centrosymmetric monoclinic space group $P2_1/c$ [No. 14; C_{2h}^5]. All 3785 unique data were corrected for the effects of absorption

Table I. Experimental Data for the X-ray Diffraction Studies of $(C_5Me_5)_2Sm[(\mu\text{-Me})AlMe_2(\mu\text{-Me})]_2Sm(C_5Me_5)_2$ (**1**) and $(C_5Me_5)_2SmMe(THF)$ (**2**)

	1	**2**
formula	$C_{48}H_{84}Al_2Sm_2$	$C_{25}H_{41}O_1Sm$
formula wt	1015.88	508.0
cryst system	monoclinic	orthorhombic
space group	$P2_1/n$	$Pnma$ (No. 62; D_{2h}^{16})
a (Å)	12.267 (3)	18.0630 (42)
b (Å)	12.575 (3)	15.6486 (39)
c (Å)	17.131 (2)	8.7678 (15)
β (deg)	100.44 (2)	
V (Å^3)	2598.7 (12)	2478.3 (10)
Z	2	4
D_{calcd} (g/cm^3)	1.30	1.36
diffractometer	Syntex $P2_1$	Syntex $P2_1$
radiation	Mo Kα (λ = 0.710730 Å)	Mo Kα (λ = 0.710730 Å)
monochromator	highly oriented graphite	highly oriented graphite
data collected	$+h,+k,\pm l$	$+h,+k,+l$
scan type	coupled θ(crystal) − 2θ(counter)	coupled θ(crystal) − 2θ(counter)
scan width	symmetrical $[2\theta(K\alpha_1) - 1.2] \rightarrow [2\theta(K\alpha_2) + 1.2]$	$[2\theta(K\alpha_1) - 1.2] \rightarrow [2\theta(K\alpha_2) + 1.2]$
scan speed in 2θ (deg min^{-1})	3.0–16.0	4.0
$2\theta_{max}$ (deg)	45.0	50.0
μ(Mo Kα) (cm^{-1})	26.3	23.9
unique reflcns	3785	2283
reflctns	2163 ($F^2 > 2.0\sigma(F^2)$)	2087 ($F^2 > 1.0\sigma(F)$)
no. of variables	185	108
R_F (%)	5.7	7.0
R_{wF} (%)	8.0	8.8
GOF	2.14	2.65

(10) For reviews containing leading references, see: Rothwell, I. P. *Polyhedron* **1985**, *4*, 177–200. Crabtree, R. H. *Chem. Rev.* **1985**, *85*, 245–269. Halpern, J. *Inorg. Chim. Acta* **1985**, *1100*, 41–48. Bergman, R. G. *Science (Washington, D.C.)* **1984**, *223*, 902–908. Shilov, A. E. *Activation of Saturated Hydrocarbons by Transition Metal Complexes*; D. Reidel: Dordrecht, Holland, 1984.

(11) Bergman, R. G.; Janowicz, A. H. *J. Am. Chem. Soc.* **1983**, *105*, 3929–3939 and references therein.

(12) Hoyano, J. K.; Graham, W. A. G. *J. Am. Chem. Soc.* **1982**, *104*, 3723–3725.

(13) Jones, W. D.; Feher, F. J. *J. Am. Chem. Soc.* **1985**, *107*, 620–631.

(14) Watson, P. L.; Parshall, G. W. *Acc. Chem. Res.* **1985**, *18*, 51–56 and references therein.

(15) Watson, P. L. *J. Am. Chem. Soc.* **1983**, *105*, 6491–6493.

(16) Thompson, M. E.; Baxter, S. M.; Bulls, A. R.; Burger, B. J.; Nolan, M. C.; Santarsiero, B. D.; Schaefer, W. P.; Bercaw, J. E. *J. Am. Chem. Soc.* **1987**, *109*, 203–219.

(17) Chamberlain, L. R.; Rothwell, I. P.; Huffman, J. C. *J. Am. Chem. Soc.* **1986**, *108*, 1502–1509.

(18) Bruno, J. W.; Smith, G. M.; Marks, T. J.; Fair, C. K.; Schultz, A. J.; Williams, J. M. *J. Am. Chem. Soc.* **1986**, *108*, 40–56.

(19) Fendrick, C. M.; Marks, T. J. *J. Am. Chem. Soc.* **1986**, *108*, 425–437.

(20) Pegg, D. T.; Doddrell, D. M.; Bendall, M. R. *J. Chem. Phys.* **1982**, *77*, 2745–2752.

(21) Evans, D. F. *J. Chem. Soc.* **1959**, 2003–2005. Becconsall, J. K. *Mol. Phys.* **1968**, *15*, 129–139.

(22) Sams, D. B.; Doedens, R. J. *Inorg. Chem.* **1979**, *18*, 153–156.

Table II. Final Fractional Coordinates for $(C_5Me_5)_2Sm[(\mu\text{-Me})AlMe_2(\mu\text{-Me})]_2Sm(C_5Me_5)_2$

atom	x	y	z
Sm(1)	0.7040 (1)	0.2048 (1)	0.4909 (1)
Al(1)	0.6728 (4)	−0.1746 (4)	0.4722 (3)
C(1)	0.7648 (49)	0.2149 (51)	0.3507 (19)
C(2)	0.7737 (28)	0.3127 (51)	0.3773 (20)
C(3)	0.6764 (54)	0.3487 (21)	0.3772 (15)
C(4)	0.6008 (20)	0.2694 (53)	0.3468 (19)
C(5)	0.6643 (67)	0.1903 (35)	0.3320 (18)
C(6)	0.8760 (38)	0.1595 (38)	0.3418 (25)
C(7)	0.8817 (40)	0.3838 (41)	0.3896 (27)
C(8)	0.6298 (43)	0.4621 (45)	0.3835 (30)
C(9)	0.4738 (40)	0.2787 (34)	0.3311 (26)
C(10)	0.6276 (47)	0.0759 (48)	0.2913 (35)
C(11)	0.7586 (23)	0.1788 (20)	0.6501 (12)
C(12)	0.7315 (17)	0.2784 (18)	0.6411 (11)
C(13)	0.8105 (27)	0.3284 (15)	0.6076 (14)
C(14)	0.8868 (17)	0.2565 (34)	0.5922 (13)
C(15)	0.8538 (31)	0.1570 (24)	0.6205 (15)
C(16)	0.6981 (25)	0.0964 (27)	0.6934 (18)
C(17)	0.6361 (28)	0.3307 (27)	0.6747 (19)
C(18)	0.8199 (27)	0.4567 (27)	0.5990 (20)
C(19)	1.0010 (31)	0.2801 (28)	0.5691 (22)
C(20)	0.9287 (30)	0.0570 (30)	0.6275 (22)
C(21)	0.5112 (13)	−0.1905 (13)	0.4865 (10)
C(22)	0.6940 (15)	−0.0133 (13)	0.4800 (11)
C(23)	0.7751 (17)	−0.2445 (17)	0.5647 (14)
C(24)	0.6876 (20)	−0.2241 (17)	0.3635 (13)

(μ = 26.3 cm^{-1}) and for Lorentz and polarization factors and reduced to unscaled $|F_o|$ values. A Wilson plot was used to place the data on an approximate absolute scale. Those 2163 data having $F^2 > 2.0\sigma F^2$ were considered observed and used in subsequent calculations.

The structure was solved by direct methods by using the program MITHRIL;[23] the position of the unique samarium atom was located from an "*E*-map." The positions of all remaining non-hydrogen atoms were determined from a series of difference-Fourier syntheses. All calculations were performed with our locally modified version of the UCLA Crystallographic Computing Package.[24] The weighting scheme employed during full-matrix least-squares refinement with $p = 0.05$ has been previously described.[25] Hydrogen atom contributions were not included in the refinement. The model converged with $R_F = 5.7\%$, $R_{wF} = 8.0\%$, and GOF = 2.14 for 185 variables refined against 2163 data (data:parameter ratio = 11.7:1). Although the C_5Me_5 rings in this structure show considerable thermal motion, the basic structure is well-defined and the bond distances and angles of the core of the structure are not affected. A final difference-Fourier map showed no significant features.

The analytical scattering factors for the neutral atoms (C, Al, Sm) were used throughout the analysis;[26a] both the real ($\Delta f'$) and imaginary ($i\Delta f''$) components of anomalous dispersion[26b] were included. Final fractional coordinates are given in Table II.

$(C_5Me_5)_2SmMe(THF)$ (2). When **1** (0.272 g, 0.26 mmol) was dissolved in 5 mL of THF in the glovebox, there was an immediate color change from orange to yellow. When this THF solution was layered with hexane (~20 mL) and cooled to −34 °C, large yellow crystals of **2** precipitated from solution. Rotary evaporation of the solvent from this solution caused **2** to revert to **1**. Therefore, to isolate **2** the solution containing the crystals must be decanted and the crystals must be quickly washed with hexane. Concentration of the decanted solution by rotary evaporation and cooling to −34 °C allows more **2** to crystallize. Overall yield: 0.112 g, 40% based on **1** used; unreacted **1** can be recovered and directly recycled. Anal. Calcd for $C_{25}H_{41}SmO$: C, 59.14; H, 8.13; Sm, 29.61. Found: C, 57.66; H, 7.56; Sm, 30.35. Magnetic susceptibility: $\chi_M^{293K} = 1050 \times 10^{-6}$ cgs; $\mu_{eff}^{293K} = 1.6\ \mu_B$. ^{1}H NMR ($C_6D_6$, 20 °C [$\Delta\nu_{1/2}$ in Hz]) 7.76 [35] (s, Sm–Me), 1.55 [13] (s, C_5Me_5), −2.28 (THF), −3.95 (THF). ^{13}C NMR (C_6D_6, 25 °C) 114.4 (by DEPT[20] techniques, Sm–Me), 114.2 (s, C_5Me_5), 59.4 (THF), 19.3 (THF), 15.6 (q, J_{CH} = 124 Hz, C_5Me_5). IR (KBr) 2850 s, 1435 m, 1378 m, 1250 w, 1172 w, 1020 m, 860 m cm^{-1}.

Table III. Final Fractional Coordinates for $(C_5Me_5)_2SmMe(THF)$

atom	x	y	z
Sm(1)	0.11435 (3)	0.25000	0.13591 (6)
C(1)	0.2068 (10)	0.25000	0.3456 (17)
C(2)	0.1243 (9)	0.4235 (9)	0.1151 (22)
C(3)	0.0944 (10)	0.4113 (8)	0.2516 (17)
C(4)	0.0214 (11)	0.3759 (8)	0.2188 (29)
C(5)	0.0158 (14)	0.3739 (11)	0.0680 (39)
C(6)	0.0798 (20)	0.4021 (11)	0.0090 (16)
C(7)	0.1981 (20)	0.4615 (22)	0.1076 (28)
C(8)	0.1255 (16)	0.4353 (22)	0.4055 (36)
C(9)	−0.0400 (23)	0.3576 (25)	0.3393 (35)
C(10)	−0.0478 (20)	0.3535 (24)	−0.0620 (42)
C(11)	0.0926 (24)	0.4187 (30)	−0.1725 (47)
C(12)	0.2928 (9)	0.25000	−0.0027 (20)
C(13)	0.3381 (11)	0.25000	−0.1431 (18)
C(14)	0.2882 (11)	0.25000	−0.2692 (20)
C(15)	0.2175 (10)	0.25000	−0.2194 (16)
O(01)	0.2163 (5)	0.25000	−0.0523 (11)

X-ray Data Collection, Structure Determination, and Refinement for 2. A bright yellow crystal of approximate dimensions 0.40 × 0.40 × 0.70 mm was mounted in a thin-walled glass capillary under nitrogen and accurately aligned on a Syntex $P2_1$ diffractometer. Subsequent setup operations (determination of accurate unit cell dimensions and orientation matrix) and collection of room temperature (22 °C) intensity data were carried out with standard techniques similar to those of Churchill.[27] Final cell parameters were based on a least-squares analysis of 25 reflections in well-separated regions of reciprocal space, all having 25° < 2θ < 34°. Details are given in Table I.

A careful survey of a preliminary data set revealed the systematic extinctions $0kl$ for $k + l = 2n + 1$ and $hk0$ for $h = 2n + 1$. The crystal belongs to the orthorhombic system; possible space groups are the noncentrosymmetric $Pn2_1a$ (a nonstandard setting of $Pna2_1$ [C_{2v}^9; No. 33]) or the centrosymmetric $Pnma$ [D_{2h}^{16}; No. 62]. With $Z = 4$ and no expectation of a resolved chiral molecule, the latter centrosymmetric space group was chosen and was later confirmed as the correct choice by successful solution of the structure.

All 2283 unique data were corrected for the effects of absorption (μ = 23.9 cm^{-1}) and for Lorentz and polarization factors and reduced to unscaled $|F_o|$ values. A Wilson plot was used to place the data on an approximate absolute scale. Those 2087 data having $F^2 > 1.0\sigma(F^2)$ were considered observed and used in subsequent calculations.

The structure was solved by direct methods with the program MITHRIL;[23] the samarium atom was located from an "*E*-map" and placed on the mirror plane corresponding to $y = {}^1/_4$. The positions of all remaining non-hydrogen atoms were determined from a series of difference-Fourier syntheses. All crystallographic calculations were performed as described above.[24,25] The structure was refined with full-matrix least-squares methods. Hydrogen atom contributions were not included in the refinement. The model converged with $R_F = 7.0\%$, $R_{wF} = 8.8\%$, and GOF = 2.65 for 108 variables refined against 2087 data (data:parameter ratio = 19.3:1). Final fractional coordinates are given in Table III.

Reactivity of $(C_5Me_5)_2SmMe(THF)$. Et_2O. The addition of two drops of Et_2O to an NMR tube containing a solution of **2** (10 mg, 0.02 mmol) in 0.45 mL of C_6D_6 caused no immediate reaction as monitored by ^{1}H NMR spectroscopy. After 24 h, a single new C_5Me_5 resonance was observed in the ^{1}H NMR spectrum at 1.42 ppm. After 72 h, the NMR was the same and the NMR tube was evacuated to remove the excess Et_2O. The remaining yellow solid was dissolved in C_6D_6 and displayed a spectrum consistent with $(C_5Me_5)_2Sm(OEt)(THF)$. ^{1}H NMR (C_6D_6, 20 °C) 5.62 (q, OCH_2CH_3), 3.29 (t, OCH_2CH_3), 1.42 (s, C_5Me_5), −2.55 (THF), −3.97 (THF). In a separate experiment, **2** (51 mg, 1.00 mmol) was allowed to react with Et_2O (0.80 mL, 7.63 mmol) in toluene for 24 h. Removal of solvent left a yellow solid (40 mg, 74%). Anal. Calcd for $SmC_{26}H_{43}O_2$: Sm, 27.95. Found: Sm, 29.6. The ^{1}H NMR spectrum was identical with that above. ^{13}C NMR (C_6D_6, 20 °C) 112.6 (s, C_5Me_5), 67.6 (t, J_{CH} = 145 Hz, OCH_2CH_3), 59.2 (THF), 20.4 (q, J_{CH} = 125 Hz, OCH_2CH_3), 16.9 (q, J_{CH} = 124 Hz, C_5Me_5).

Pyridine. An NMR tube containing **2** (ca. 20 mg, ca. 0.04 mmol) was attached to a vacuum line and evacuated. Pyridine-d_5 was condensed into the tube and the tube was sealed. A ^{1}H NMR spectrum was immediately taken and showed the presence of CH_3D (0.106 ppm, t, J_{HD} = 1.9 Hz), free THF at 1.62 and 3.68 ppm, and two C_5Me_5 resonances at 1.11 and

(23) Gilmore, C. J. *J. Appl. Cryst.* **1984**, *17*, 42–46.
(24) UCLA Crystallographic Computing Package, University of California, Los Angeles, 1981. Strouse, C., personal communication.
(25) Corfield, P. W. R.; Doedens, R. J.; Ibers, J. A. *Inorg. Chem.* **1967**, *6*, 197–204.
(26) *International Tables for X-ray Crystallography*; Kynoch Press: Birmingham, England, 1974; Vol. IV, p 72: (a) pp 99–101; (b) pp 145–150.
(27) Churchill, M. R.; Lashewycz, R. A.; Rotella, F. J. *Inorg. Chem.* **1977**, *16*, 265–271.

1.52 ppm. Within 15 min the 1.52 peak of **2** had disappeared leaving only the 1.11 peak. After 24–48 h, two new resonances appeared in the ^{1}H NMR spectrum at 0.91 and 0.96 ppm and over a 1–2 week period their intensity grew as that of the 1.11 peak diminished until all three peaks were equal in size. The solution turned dark red-brown during this time and yet another peak appeared at 2.52 ppm. Upon heating this sample to 75 °C, further changes occurred. After 3 h, peaks at 1.02 and 1.15 ppm were observed in addition to all of those above. After 24 h at 75 °C, the ^{1}H NMR spectrum contained just the resonances at 1.02, 1.15, and 2.52 ppm in the ratio of 1:1.6:5, respectively.

C_6D_6. A solution of **2** (11 mg, 0.021 mmol) in ~0.45 mL of C_6D_6 was prepared in an NMR tube. The tube was attached to a vacuum line, cooled in a liquid nitrogen bath, evacuated, and sealed. After 24 h at room temperature, methane and $(C_5Me_5)_2Sm(C_6D_5)(THF)$ (identified by comparison with the ^{1}H NMR spectrum of $(C_5Me_5)_2Sm(C_6H_5)(THF)$[28]) were observed. The ratio of **2** to $(C_5Me_5)_2Sm(C_6D_5)(THF)$ was 2.4. This ratio changed with time: 72 h, 0.9; 120 h, 0.3. After 6 days, **2** had completely converted to the phenyl complex and methane.

Toluene. In the glove box, **2** (48 mg, 0.094 mmol) was dissolved in 10 mL of toluene. The solution changed from bright yellow to dark brown as it was stirred over a 5-day period. Removal of solvent by rotary evaporation left a red-brown oil. Addition of THF and solvent removal gave a red-brown solid (47 mg, 74%) identified as $(C_5Me_5)_2Sm(CH_2C_6H_5)(THF)$ by comparison of its ^{1}H NMR spectrum with that of a crystallographically characterized sample.[29] ^{1}H NMR (C_6D_6, 25 °C [$\Delta\nu_{1/2}$ in Hz]) 10.31 [56] (br, s, CH_2Ph), 7.6–6.2 (m, CH_2Ph), 1.32 [4] (s, C_5Me_5), −1.29 [16] (br s, THF), −1.97 [24] (br s, THF).

A reaction with $C_6D_5CD_3$ was monitored by ^{1}H NMR spectroscopy with **2** (8 mg, 0.016 mmol) in 0.45 mL of toluene-d_8. After 24 h, methane and **2** and $(C_5Me_5)_2Sm(CD_2C_6D_5)(THF)$ were observed. The latter two compounds were present in a relative ratio of 1:6, respectively. This ratio changed with time: 48 h, 3:1; 72 h, 1:1.5; 120 h, 1:2; 216 h, 1:10.

C_6D_{12}. A sealed NMR sample of **2** (15 mg, 0.03 mmol) in 0.45 mL of C_6D_{12} was prepared as described above. The ^{1}H NMR spectrum taken immediately after sample preparation showed the presence of only **2**. Within 24 h, the C_5Me_5 resonance of **2** was gone and four new peaks in the 0.90–1.65 ppm range were observed along with a peak for methane. After 48 h, these four peaks were gone and four entirely different peaks were observed in the 0.90–1.65 ppm region and the spectrum continued to change over a 2-week period.

Cyclooctane. **2** (15 mg, 0.03 mmol) was dissolved in 7 mL of cyclooctane and stirred for 6 days. Removal of solvent by rotary evaporation gave a yellow oil. The ^{1}H NMR spectrum of the oil in C_6D_6 contained resonances at 1.49, 1.41, 1.31, and 1.28 ppm in the ratio 6:1:1:1, respectively.

Hydrogen. A suspension of **2** (27 mg, 0.053 mmol) in 10 mL of hexane was stirred under an atmosphere of H_2 for 80 h at room temperature. An orange solid precipitated from solution. It was filtered, washed with hexane, and identified by ^{1}H NMR spectroscopy as $[(C_5Me_5)_2Sm(\mu\text{-}H)]_2$[30] (19 mg, 85%).

Ethylene Polymerization. A solution of **1** (20 mg, 0.02 mmol) in 5 mL of toluene [0.008 M in Sm] was placed in a 3-oz Fischer–Porter aerosol reaction vessel fitted with a pressure gauge. Ethylene was added until a pressure of 30 psi was reached and the valve to the system was closed. White solid polyethylene began to form immediately, and all of the monomer was consumed in 9 min. Filtration of the solution followed by drying the white solid gave polyethylene. The polymer was not soluble enough in trichlorobenzene to get a molecular weight distribution.

A 0.008 M solution of **2** was treated similarly with ethylene. The ethylene was consumed in 15 min. The weight average and number average molecular weights were 242 000 and 67 000, respectively. A 0.008 M solution of $(C_5Me_5)_2Sm(\mu\text{-}Et)_2AlEt_2$[31] was also reacted with ethylene under the same conditions. Complete ethylene consumption required 15 h. The weight average and number average molecular weights were 483 000 and 4 000, respectively.

Kinetic Measurements of Intermolecular C–H and C–D Activation by 2. Four NMR tubes containing a 0.048 M solution of **2** in benzene-d_6 were sealed under vacuum. Experiments were carried out at 55, 65, 75, and 85 °C in the NMR probe, allowing for equilibration time of the probe (15 min) with the sample removed, and also for equilibration of the sample (~5 min). The kinetics of **2** converting to **5** were monitored by ^{1}H NMR by observing the increase in the intensity of the C_5Me_5 peak of **5**. At 75 and 85 °C the reaction was monitored over 5 half-lives, and at 55 and 65 °C over 4 half-lives. Plots of ln [**5**] versus time were linear over 4 half-lives. The slope of each line was the rate constant, k, at each given temperature. Plotting ln k/T versus $1/T$ (K) gives a straight line from which the slope and intercept can be used to determine $\Delta H^\ddagger$ and $\Delta S^\ddagger$ with the equation $K = (RT/Nh)\exp(\Delta S^\ddagger/R) - \exp(-\Delta H^\ddagger/RT)$.[32]

Attempts to study the dependence of this reaction on the concentration of benzene with C_6D_{12} as a solvent were complicated by the reactivity of **2** with C_6D_{12}. Samples of **2** in C_6D_{12} containing varying measured amounts of C_6H_6 were monitored by ^{1}H NMR spectroscopy over several days. Initially the ^{1}H NMR spectrum of each sample contained peaks for only **2** (1.46 ppm C_5Me_5), C_6H_6, and a residual proton peak for cyclohexane-d_{12}. Within 12 h the peak for **2** disappeared, a peak for methane was present, and there were four to six new resonances in the 0.9–1.65 ppm range (the number depended on the C_6H_6 concentration). The spectra were monitored again after 24 h, 36 h, and 6 days. At least 15 peaks were observed in the 0.9–1.65 ppm region which varied with time and C_6H_6 concentration in a complicated way.

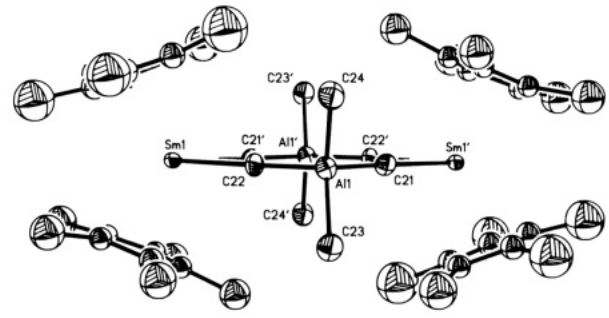

Figure 1. Molecular structure of $(C_5Me_5)_2Sm[(\mu\text{-}Me)AlMe_2(\mu\text{-}Me)]_2Sm(C_5Me_5)_2$ (**1**).

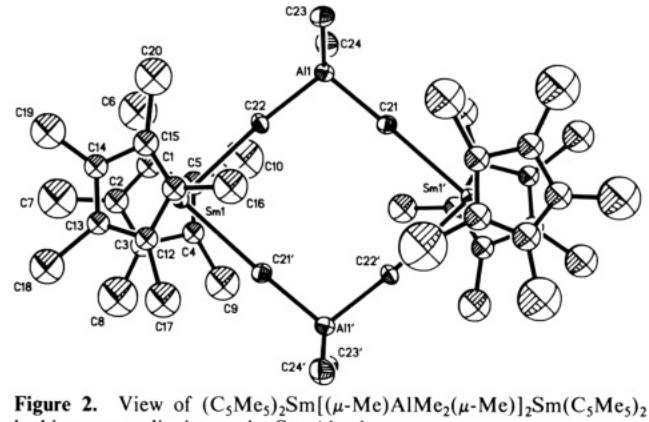

Figure 2. View of $(C_5Me_5)_2Sm[(\mu\text{-}Me)AlMe_2(\mu\text{-}Me)]_2Sm(C_5Me_5)_2$ looking perpendicular to the Sm_2Al_2 plane.

Results

Synthesis and X-ray Crystal Structure of $(C_5Me_5)_2Sm[(\mu\text{-}Me)AlMe_2(\mu\text{-}Me)]_2Sm(C_5Me_5)_2$ (1). The purple divalent samarium complex $(C_5Me_5)_2Sm(THF)_2$[2] reacts with an excess of $AlMe_3$ to afford a red-orange solution and a finely divided black precipitate. After the precipitate was separated by decanting and filtering, the solvent was removed from the filtrate to yield **1** as a red-orange solid. The NMR spectra of crystals of **1** were complicated (see below) and hence an X-ray study was performed to identify this complex. Complex **1** crystallizes from toluene at low temperature as the dimer $(C_5Me_5)_2Sm[(\mu\text{-}Me)AlMe_2(\mu\text{-}Me)]_2Sm(C_5Me_5)_2$. Two views of this molecule are shown in Figures 1 and 2. Selected bond distances and angles are given in Table IV. These data are consistent with the synthesis of **1** according to eq 1.

$$2(C_5Me_5)_2Sm(THF)_2 + \text{excess } AlMe_3 \rightarrow (C_5Me_5)_2Sm[(\mu\text{-}Me)AlMe_2(\mu\text{-}Me)]_2Sm(C_5Me_5)_2 + Al + THF \quad (1)$$

(28) Evans, W. J.; Bloom, I.; Hunter, W. E.; Atwood, J. L. *Organometallics* **1985**, *4*, 112–119.
(29) Evans, W. J.; Ulibarri, T. A.; Doedens, R. J., unpublished results.
(30) Evans, W. J.; Bloom, I.; Hunter, W. E.; Atwood, J. L. *J. Am. Chem. Soc.* **1983**, *105*, 1401–1403.
(31) Evans, W. J.; Chamberlain, L. R.; Ziller, J. W. *J. Am. Chem. Soc.* **1987**, *109*, 7209–7211.
(32) Espenson, J. H. *Chemical Kinetics and Reaction Mechanisms*; McGraw-Hill: New York, 1981.

Table IV. Selected Interatomic Bond Distances (Å) and Angles (deg) for $(C_5Me_5)_2Sm[(\mu\text{-Me})AlMe_2(\mu\text{-Me})]_2Sm(C_5Me_5)_2$[a]

Sm(1)–C(1)	2.644 (28)	Sm(1)–C(15)	2.681 (19)
Sm(1)–C(2)	2.639 (22)	Sm(1)–C(21)′	2.743 (16)
Sm(1)–C(3)	2.635 (21)	Sm(1)–C(22)	2.750 (16)
Sm(1)–C(5)	2.683 (31)	Sm(1)–Cent(1)	2.414
Sm(1)–C(4)	2.688 (20)	Sm(1)–Cent(2)	2.419
Sm(1)–C(11)	2.708 (19)	Al(1)–C(21)	2.051 (17)
Sm(1)–C(12)	2.698 (17)	Al(1)–C(22)	2.046 (17)
Sm(1)–C(13)	2.678 (18)	Al(1)–C(23)	2.034 (20)
Sm(1)–C(14)	2.656 (20)	Al(1)–C(24)	2.003 (21)
C(21)′–Sm(1)–C(22)	85.0 (5)	Cent(1)–Sm(1)–Cent(2)	138.6
C(21)′–Sm(1)–Cent(1)	106.4	C(21)–Al(1)–C(22)	101.7 (7)
C(21)′–Sm(1)–Cent(2)	103.9	C(21)–Al(1)–C(23)	109.8 (8)
C(22)–Sm(1)–Cent(1)	105.4	C(21)–Al(1)–C(24)	109.5 (9)
C(22)–Sm(1)–Cent(2)	104.7	C(22)–Al(1)–C(23)	108.9 (9)
Sm(1)–C(21)′–Al(1)′	177.8 (7)	C(22)–Al(1)–C(24)	109.7 (9)
Sm(1)–C(22)–Al(1)	175.2 (9)	C(23)–Al(1)–C(24)	116.3 (10)

[a] Cent is the centroid of the pentamethylcyclopentadienyl ring.

The structure of **1** contains two typical trivalent $(C_5Me_5)_2Sm$ bent metallocene units, each of which is coordinated to two additional ligands to form formally eight-coordinate samarium centers. The average Sm–C(C_5Me_5 ring) distance of 2.675 (1) Å, the (ring centroid)–Sm–(ring centroid) angle of 138.6°, and the staggered arrangement of the C_5Me_5 rings[33] are all normal for trivalent $(C_5Me_5)_2Sm$ complexes.[34,35]

Similarly, the overall geometry around aluminum is normal for a Me_4Al^- species.[36,37] The four methyl groups form a roughly tetrahedral environment around the aluminum atom. The C–Al–C angles average 109° and four of these angles are within 1° of this value. The C(21)–Al–C(22) angle involving the bridging methyl groups is smaller, 101.7 (7)°, and the C(23)–Al–C(24) angle involving only terminal carbons is larger, 116.3 (10)°. Variations of this magnitude are not uncommon in the structures of Me_4Al^- complexes.[36,37]

The average distance from Al to the bridging carbon atoms, C(21) and C(22), 2.049 (12) Å, is slightly longer than the average Al to terminal carbon distance, 2.019 (14) Å. This is typical of organoaluminum complexes. For example, $Me_2Al(\mu\text{-Me})_2AlMe_2$ has an average Al–C(bridging) distance of 2.124 (2) Å, and an average Al–C(terminal) distance of 1.952 (4) Å.[38] $(C_5H_5)_2Yb(\mu\text{-Me})_2AlMe_2$ has an Al–C(bridging) distance of 2.14 (2) Å and an Al–C(terminal) distance of 1.99 (2) Å.[39] Methylaluminum complexes typically have Al–C(terminal methyl) distances in the 1.95–2.01 Å range.[40,41] Hence, the Al–C(terminal) distances in **1** appear to be normal and the Al–C(bridging) distance may be a little shorter than would be expected.

The average Sm–C(bridging methyl) distance of 2.75 (1) Å is not unusual when compared with the Sm–C(terminal methyl) distance of 2.484 (14) Å in $(C_5Me_5)_2SmMe(THF)$ (**2**) (see below) and when this pair of distances is compared with other pairs of similar organolanthanide complexes which contain the same ligand in bridging and terminal positions. The best set of complexes for

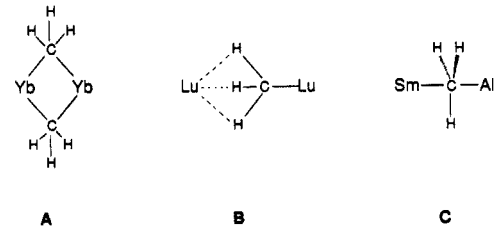

Figure 3. Possible hydrogen arrangements for bridging methyl ligands.

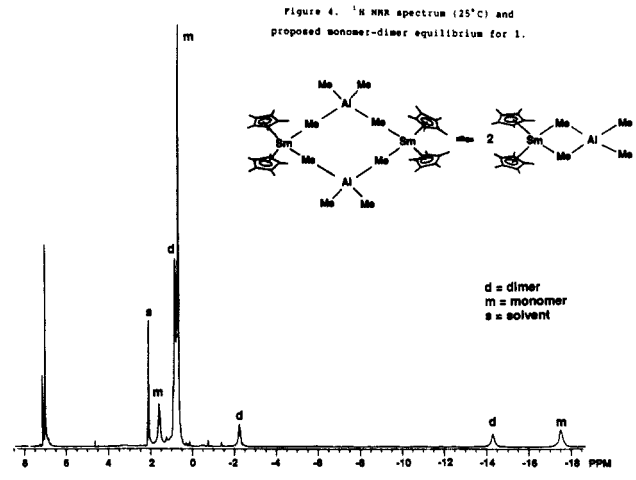

Figure 4. ^1H NMR spectrum (25 °C) and proposed monomer–dimer equilibrium for **1**.

comparison is $(C_5H_5)_2Yb(\mu\text{-Me})_2AlMe_2$ (**3**)[39] and $(C_5H_5)_2YbMe(THF)$ (**4**).[42] The former complex has an Yb–C(bridging methyl) distance of 2.58 (3) Å and the latter complex has an Yb–C(terminal methyl) distance of 2.36 (1) Å. The difference in the Yb–C distances, 0.22 Å, is comparable to the difference in the Sm–C distances in **1** and **2**, 0.27 Å. Comparisons can also be made with eight coordinate organolanthanide chloride complexes that have Ln–Cl(bridging) distances ranging from 0.05 to 0.20 Å longer than Ln–Cl(terminal) distances.[43] It should be noted that the Sm–C(methyl) distances in **1** and **2** are larger than the analogous Yb–C(methyl) distances in **3** and **4** by 0.12–0.17 Å. This is slightly more than the 0.094[44]–0.106 Å[45] difference in the radii of the metals, but this may be due to the steric differences in the cyclopentadienyl groups.

What is unusual in the structure of **1** is the nearly linear Al–C–Sm angles of 175.2 (9) and 177.8 (7)°. This type of methyl bridging geometry differs greatly from that in $(C_5H_5)_2Yb(\mu\text{-Me})_2AlMe_2$[39] in which the Al–C–Yb angles are 77.7 (7) and 80.0 (6)°. Large Ln–(bridging ligand)–Ln angles are well-documented for chloride ligands in $(C_5Me_5)_2ClY(\mu\text{-Cl})Y(C_5Me_5)_2$,[43] 162.8 (2)°, $(C_5Me_5)_2ClSm(\mu\text{-Cl})Sm(tetraglyme)(C_5Me_5)_2$,[34] 164.8 (4)°, and $[(C_5Me_5)_2ClSm]_2(\mu\text{-Cl})^-$,[34] 165.1 (4)°, and a Lu–C–Lu angle of 170 (4)° has been cited for $(C_5Me_5)_2MeLu(\mu\text{-Me})Lu(C_5Me_5)_2$.[46] However, metal–(bridging methyl carbon)–*Al* angles of the magnitude observed for **1** are rare.[47,50]

(33) The twist angle, defined as the average of the five smallest dihedral angles formed between the ten planes which consist of a ring carbon and the two ring centroids, is 30.8°.

(34) Evans, W. J.; Drummond, D. K.; Grate, J. W.; Zhang, H.; Atwood, J. L. *J. Am. Chem. Soc.* **1987**, *109*, 3928–3936 and references therein.

(35) Evans, W. J.; Hanusa, T. P.; Levan, K. R. *Inorg. Chim. Acta* **1985**, *110*, 191–195 and references therein.

(36) Wolfrum, R.; Sauermann, G.; Weiss, E. *J. Organomet. Chem.* **1969**, *18*, 27–47.

(37) Atwood, J. L.; Hrncir, D. C. *J. Organomet. Chem.* **1973**, *61*, 43–48.

(38) Huffman, J. C.; Streib, W. E. *J. Chem. Soc., Chem. Commun.* **1971**, 911–912.

(39) Holton, J.; Lappert, M. F.; Ballard, D. G. H.; Pearce, R.; Atwood, J. L.; Hunter, W. E. *J. Chem. Soc., Dalton Trans.* **1979**, 45–53.

(40) Eisch, J. J. In *Comprehensive Organometallic Chemistry*; Wilkinson, G.; Stone, F. G. A., Abel, E. W., Eds.; Pergamon: New York, 1982; Chapter 6 and references therein.

(41) Isostructural $K[AlMe_4]$, $Rb[AlMe_4]$, and $Cs[AlMe_4]$ were reported to have Al–C distances of 2.10 (10), 2.06 (10), and 1.95 (20) Å, but the quality of the data limited the statistical significance of these measurements.[36] A better data set on the Rb complex indicated that Al–C was 2.006 (8) Å.[37]

(42) Evans, W. J.; Dominguez, R.; Hanusa, T. P. *Organometallics* **1986**, *5*, 263–270.

(43) Evans, W. J.; Peterson, T. T.; Rausch, M. D.; Hunter, W. E.; Zhang, H.; Atwood, J. L. *Organometallics* **1985**, *4*, 554–559.

(44) Shannon, R. D. *Acta Crystallogr., Sect. A: Cryst. Phys., Diffr. Theor. Gen. Crystallogr.* **1976**, *A32*, 751–767.

(45) Cotton, F. A.; Wilkinson, G., *Advanced Inorganic Chemistry*, 4th ed.; Wiley: New York, 1980.

(46) Watson, P. L.; Calabrese, J. C., to be published results cited in ref 14.

(47) X-ray data on an yttrium analogue of **1** were presented[48] at a meeting[1] but were regarded as preliminary due to poor crystal quality. Since this paper on **1** was submitted, these results have been published.[49]

(48) Busch, M. A.; Watson, P. L., unpublished results cited by Watson, P. L at the 2nd International Conference on the Basic and Applied Chemistry of f-Transition (Lanthanide and Actinide) and Related Elements, Lisbon Portugal, April 1987, L(IV)4.

The nearly linear Sm–C–Al angle raises interesting questions regarding the position of the hydrogen atoms of the bridging methyl group. Unfortunately, these could not be located in the X-ray study. The large angle precludes the hydrogen arrangement found for bent bridge systems (Figure 3A) as in $[(C_5H_5)_2Y(\mu\text{-}Me)]_2$.[51] The normal Sm–C and Al–C distances argue against the hydrogen-bridged structure proposed for $(C_5Me_5)_2MeLu(\mu\text{-}Me)Lu(C_5Me_5)_2$[46] (Figure 3B). A structure in which the hydrogen atoms occupy the equatorial positions of a trigonal bipyramid (with Sm and Al at the axial positions, Figure 3C) seems most reasonable.[52]

NMR Spectroscopy of 1. The ^1H NMR spectrum of **1** in toluene-d_8 (Figure 4) is more complex than that expected on the basis of the solid-state structure. Twice as many C_5Me_5 and methyl resonances are observed and variable-temperature NMR studies show that these fall into two sets that interconvert. The δ 0.87 C_5Me_5 resonance is associated with the δ −2.26 and −14.3 methyl resonances and the complex giving these resonances is called **1a**. The 0.69 C_5Me_5 resonance is associated with the 1.63 and −17.6 methyl resonances and this complex is called **1b**. The resonances most strongly shifted upfield, −14.3 and −17.5, can be assigned to the bridging methyl groups, which are the methyl moieties closest to the paramagnetic samarium center (μ_{eff} = 1.6 μ_B). The other methyl resonances are presumably due to the terminal methyl groups on aluminum. The ratio of **1a** to **1b** is 2.5 at −15 °C, 0.45 at room temperature, and 0.2 at 45 °C. These data are consistent with a monomer–dimer equilibrium as shown in eq 2 in which **1a** is the dimer. This equilibrium was studied

$$\underset{\mathbf{1a}}{(C_5Me_5)_2Sm[(\mu\text{-}Me)AlMe_2(\mu\text{-}Me)]_2Sm(C_5Me_5)_2} \rightleftharpoons 2\underset{\mathbf{1b}}{(C_5Me_5)_2Sm(\mu\text{-}Me)_2AlMe_2} \quad (2)$$

from −15 to 55 °C in 10-deg increments to obtain the thermodynamic parameters of this interconversion (temperatures lower than −20 °C cause **1** to precipitate from solution). From the plot of ln K_{obsd} versus T with $K_{obsd} = [\mathbf{1b}]^2/[\mathbf{1a}]$, a $\Delta H°$ of 8.7 ± 0.5 kcal and a $\Delta S°$ of 24 ± 2 eu were obtained. These $\Delta H°$ and $\Delta S°$ values are comparable to those obtained for the monomer–dimer equilibria postulated for the Y[48,49,53] and Lu[54] analogues of **1**.

The room temperature ^{13}C NMR spectrum of **1** contained four C_5Me_5 resonances consistent with the **1a** ⇌ **1b** equilibrium, but no methyl signals were observed. Variable-temperature studies indicated that the 119.2- and 19.8-ppm signals arose from the C_5Me_5 and $C_5\mathit{Me}_5$ carbons, respectively, of dimeric **1a**. The 118.4- and 18.9-ppm signals were due to the analogous resonances of monomeric **1b**.

Synthesis and NMR Spectra of $(C_5Me_5)_2SmMe(THF)$. When orange crystals of **1** were dissolved in THF, a yellow solution formed. Removal of solvent left an orange solid that was identified as **1** by ^1H NMR spectroscopy in C_6D_6. Addition of THF to the orange solid once again generated a yellow solution. Layering the THF solution with hexane and cooling to −34 °C yielded yellow X-ray quality crystals of **2** that were identified by NMR spectroscopy and X-ray crystallography as $(C_5Me_5)_2SmMe(THF)$.

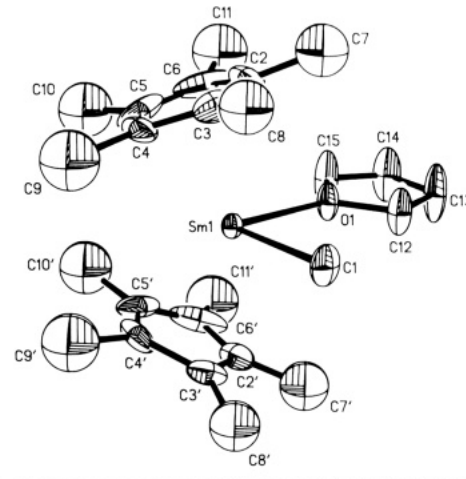

Figure 5. Molecular structure of $(C_5Me_5)_2SmMe(THF)$ (**2**).

Table V. Selected Interatomic Bond Distances (Å) and Angles (deg) for $(C_5Me_5)_2SmMe(THF)$[a]

Sm(1)–C(1)	2.484 (14)	Sm(1)–C(5)	2.698 (15)
Sm(1)–C(2)	2.726 (14)	Sm(1)–C(6)	2.701 (14)
Sm(1)–C(3)	2.744 (12)	Sm(1)–O(1)	2.473 (9)
Sm(1)–C(4)	2.688 (12)	Sm(1)···Cent	2.458
O(1)–Sm(1)–C(1)	89.6 (5)	C(1)–Sm–Cent	104.0
O(1)–Sm–Cent	104.5	C(12)–O(1)–Sm(1)	120.7 (9)
Cent–Sm(1)–Cent′	139.4	C(15)–O(1)–Sm(1)	132.7 (8)

[a] Cent is the centroid of the pentamethylcyclopentadienyl ring.

The synthesis of **2** is consistent with the equilibrium shown in eq 3.

$$(C_5Me_5)_2Sm[(\mu\text{-}Me)AlMe_2(\mu\text{-}Me)]_2Sm(C_5Me_5)_2 + 4THF \rightleftharpoons 2(C_5Me_5)_2SmMe(THF) + 2AlMe_3(THF) \quad (3)$$

Complex **2** is slightly soluble in hexane and very soluble in benzene and toluene. The ^1H NMR spectrum of the paramagnetic **2** (μ_{eff} = 1.6 μ_B) in C_6D_6 exhibited a resonance attributable to the C_5Me_5 methyl group at δ 1.55 and a resonance at δ 7.66 attributable to the methyl group attached to samarium. THF peaks were found at −2.28 and −3.95 ppm, which is typical of $(C_5Me_5)_2SmQ(THF)$ complexes (Q = Ph, Cl, I).[28,34,56] The ^{13}C NMR spectrum of **2** contained signals for C_5Me_5 (15.5, 114.2 ppm) and THF (19.3, 59.4 ppm) in the normal region, but it did not reveal a Sm–Me resonance. With use of DEPT pulsing sequences,[20] it was found that the Sm–Me peak occurred at 114.4 ppm and was partially obscured by the C_5Me_5 peak in the normal ^{13}C NMR spectrum.

X-ray Crystal Structure of $(C_5Me_5)_2SmMe(THF)$. The structure of **2**, the first X-ray crystal structure of a samarium complex containing a terminal methyl ligand,[9] is shown in Figure 5. The samarium atom in **2** occupies a special position on a mirror plane across which the THF molecule is disordered. Hence, the THF is not really planar as shown by the average of THF positions in Figure 5. There is also rotational disorder in the C_5Me_5 rings that could not be resolved with an idealized disorder model. Hence, the ring positions in Figure 5 are averages and the X-ray data do not show them to be eclipsed. Selected bond distances and angles are given in Table V.

The overall structure of **2** is typical of a bent metallocene with two additional ligands and the bonding parameters are similar to those in $(C_5Me_5)_2Sm(C_6H_5)(THF)$ (**5**),[28] $(C_5Me_5)_2Sm(CH_2C_6H_5)(THF)$ (**6**),[29] $(C_5Me_5)_2SmCl(THF)$ (**7**),[56] and $(C_5Me_5)_2SmI(THF)$ (**8**).[56] Hence, the average Sm–C(C_5Me_5 ring) distance of 2.711 (6) Å is similar to the 2.74 (1), 2.755 (2), 2.72 (3), and 2.725 (1) Å distances in **5**–**8**, respectively. The (ring centroid)–Sm–(ring centroid) angle in **2**, 134.9°, is within the 133–137° range of values found in **5**–**8** as is the Sm–O(THF)

(49) Busch, M. A.; Harlow, R.; Watson, P. L. *Inorg. Chim. Acta* **1987**, *140*, 15–20.

(50) A few near linear methyl bridges involving other elements have been reported. Li–Me–B: Rhine, W. E.; Stucky, G.; Peterson, S. W. *J. Am. Chem. Soc.* **1975**, *97*, 6401–6406. Zr–Me–Zr: Waymouth, R. M.; Santarsiero, B. D.; Grubbs, R. H. *J. Am. Chem. Soc.* **1984**, *106*, 4050–4051. Lu–Me–Lu,[46] Yb–Me–Be: Burns, C. J.; Andersen, R. A. *J. Am. Chem. Soc.* **1987**, *109*, 5853–5855.

(51) Holton, J.; Lappert, M. F.; Ballard, D. G. H.; Pearce, R.; Atwood, J. L.; Hunter, W. E. *J. Chem. Soc., Dalton Trans.* **1979**, 54–61.

(52) Coupling constant arguments have been made to support a Figure 3c structure for the yttrium analogue of **1**.[48,49] Similar data are not available for **1** due to the presence of the paramagnetic metal center.

(53) Teuben, J. H.; den Haan, K. H., personal communication. den Haan, K. H. Ph.D. Thesis, University of Groningen, 1986.

(54) Monomeric $(C_5Me_5)_2Ln(\mu\text{-}Me)_2AlMe_2$ complexes have been described for Ln = Yb, Lu.[14,55] A monomer dimer equilibrium for Ln = Lu subsequently was described.[48,49]

(55) Watson, P. L.; Herskovitz, T. *ACS Symp. Ser.* **1983**, *212*, 459–479.

(56) Evans, W. J.; Grate, J. W.; Levan, K. R.; Bloom, I.; Peterson, T. T.; Doedens, R. J.; Zhang, H.; Atwood, J. L. *Inorg. Chem.* **1986**, *25*, 3614–3619.

Table VI. Observed Rate Constants for the Reaction of $(C_5Me_5)_2SmMe(THF)$ (**2**) with C_6D_6[a]

T (°C)	10^3k	$t_{1/2}$ (min)
55	3.41	203
65	8.23	83
75	18.4	37
85	31.4	21

[a] For 0.048 M solutions of **2** in C_6D_6. $-d[\mathbf{2}]/dt = k_{obsd}[\mathbf{2}]$.

distance of 2.473 (9) Å (compared to 2.44 (2)–2.511 (4) Å in **5**–**8**). The Sm–C(methyl) distance of 2.484 (14) Å is not significantly different from the 2.511 (8) Å Sm–C(phenyl) distance in **5** and the 2.498 (5) Å Sm–C(benzyl) distance in **6**.

Recently we learned that the structure of $(C_5Me_5)_2YMe(THF)$ (**9**) had also been determined.[53,57] Complexes **2** and **9** are isostructural. The average Y–C(ring) distance of 2.66 (5) Å, the Y–C(methyl) distance of 2.44 (2) Å, and the Y–O(THF) distance of 2.379 (8) Å are 0.04–0.10 Å shorter than those of **2** due to the smaller atomic radius of Y^{3+} compared to Sm^{3+}. The radial difference between these ions is 0.06[44]–0.084[45] Å. Adding these numbers to the distances of **9** gives distances the same as those in **2** within a few hundredths of an angstrom.[58]

Complex **9** is thought to have agostic[59] methyl C–H–Y interactions on the basis of a lowered ν_{CH} absorption at 2770 cm^{-1} and a 108.2 Hz average J_{CH} coupling constant for the methyl group. The disorder in the X-ray structure of **9** complicated attempts to show this agostic interaction in the solid state.

An agostic methyl hydrogen interaction might be even more likely to occur in **2** than in **9** to help compensate for the fact that the larger samarium metal center in **2** is less sterically saturated.[4,60] However, the paramagnetic nature of Sm^{3+} complicates the NMR analysis of such an interaction and the IR spectrum shows only a small absorption at 2720 cm^{-1} which is higher than the 2700–2350 cm^{-1} range normally found in fully defined agostic systems.[59,61] Nevertheless, the potential for such an agostic interaction exists in **2**.

Reactivity of 2. Although **2** is thermally stable at room temperature, it decomposes upon heating both in solution and in the solid state. Attempts to sublime or desolvate **2** by heating under vacuum were unsuccessful. Heating **2** to 62 °C for 4 h at 10^{-6} Torr produced no visible change and no pressure surge due to THF loss.[63] At 80 °C, **2** decomposed over a 4-h period to give brown insoluble materials. The thermal decomposition of **2** at 76 °C in THF was monitored over a period of several days by ^1H NMR spectroscopy in sealed NMR tubes. The decomposition was complex: several different resonances were observed in the C_5Me_5 region which changed in intensity during the course of the reaction. No evidence of methane formation was observed.

THF is the only common solvent we have found so far with which **2** does not react at room temperature. **2** has been observed to react with all of the following species: Et_2O, pyridine, toluene, benzene, hexane, cyclohexane, and cyclooctane. The latter three solvents react with **2** to form methane and complicated mixtures of reactive organosamarium species[65] which change in composition

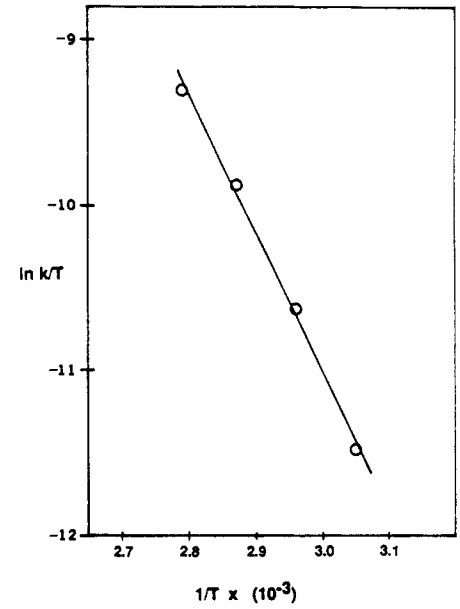

Figure 6. Activated complex plot for $(C_5Me_5)_2SmMe(THF) + C_6D_6 \rightarrow (C_5Me_{5-x}(d_x))_2Sm(C_6D_5)(THF)$.

over periods as long as 2 weeks. The reactions of **2** with Et_2O, benzene, and toluene are more specific and have allowed for definitive characterization of the products. Addition of Et_2O to a benzene solution of **2** does not cause an immediate reaction. However, over a 24-h period **2** is converted cleanly to $(C_5Me_5)_2Sm(OEt)(THF)$, which was identified by ^1H and ^{13}C NMR spectroscopy and complexometric metal analysis.

2 reacts with C_6D_6 to form $(C_5Me_5)_2Sm(C_6D_5)(THF)$[28] (**10**) and methane in quantitative yield (eq 4). The reaction is 30%

$$(C_5Me_5)_2SmMe(THF) + C_6D_6 \rightarrow (C_5Me_{5-x}(d_x))_2Sm(C_6D_5)(THF) + CH_4 \quad (4)$$

complete after 24 h at room temperature and is complete after 6 days. ^1H and ^{13}C NMR analysis of the methane generated showed it to be CH_4 not CH_3D. The kinetics of the reaction of **2** with C_6D_6 were studied under pseudo-first-order conditions in C_6D_6 in sealed NMR tubes over the temperature range of 55–85 °C by monitoring the C_5Me_5 resonance of $(C_5Me_5)_2Sm(C_6D_5)(THF)$ (**10**). Plots of ln [**10**] versus time were found to be linear over 4 half-lives. The rate constant data are given in Table VI and a plot of ln k_{obsd}/T versus T^{-1} is shown in Figure 6. From this plot a $\Delta H^{\ddagger}$ of 16.5 ± 0.6 kcal and a $\Delta S^{\ddagger}$ of −19 ± 4 eu were calculated.

The dependence of the reaction rate on the benzene concentration was not readily determined. In THF, the reactivity of **2** with benzene is severely inhibited. Hence, an NMR sample of **2** in THF-d_8:benzene (10:1) showed no $(C_5Me_5)_2Sm(C_6H_5)(THF)$ formation after 17 days. Only a small amount of $(C_5Me_5)_2Sm(C_6H_5)(THF)$ was detectable after 29 days. In C_6D_{12}, the reactivity of **2** with benzene is extremely complex. Numerous C_5Me_5 resonances appeared in the ^1H NMR spectrum and were observed to vary in intensity over a several day period.

Complex **2** reacts with toluene to form $(C_5Me_5)_2Sm(CH_2C_6H_5)(THF)$ according to eq 5. The benzyl complex is the

$$(C_5Me_5)_2SmMe(THF) + C_6H_5CH_3 \rightarrow (C_5Me_5)_2Sm(CH_2C_6H_5)(THF) + CH_4 \quad (5)$$

exclusive product of this reaction, and no evidence for tolyl derivatives was observed at room temperature. Consistent with this, a sample of **2** in benzene-d_6:toluene (10:1) generated only the benzyl product over a 1-day period. Small amounts of $(C_5Me_5)_2Sm(C_6D_5)(THF)$ were subsequently formed.

In contrast to the above reactions, **2** generates CH_3D when treated with pyridine-d_5. The reaction is so fast that unless the two components are put together at low temperature and sealed, the CH_3D generated will not be observed. The initially observed

(57) den Haan, K. H.; De Boer, J. L.; Teuben, J. H.; Smeets, W. J. J.; Spek, A. L. *J. Organomet. Chem.* **1987**, *327*, 31–38.
(58) Some preliminary bond distances on the Yb analogue of **2** and **9** have been given in a figure[55] that are also consistent with the values found for **2** and **9**.
(59) Brookhart, M.; Green, M. L. H. *J. Organomet. Chem.* **1983**, *250*, 395–408.
(60) Evans, W. J. *Adv. Organomet. Chem.* **1985**, *24*, 131–177.
(61) Infrared ν_{CH} absorptions at no lower than 2720 cm^{-1} are also observed for $(C_5Me_5)_2YN(SiMe_3)_2$ and $(C_5Me_5)_2YCH(SiMe_3)_2$, which both contain agostic Y–H interactions.[62]
(62) den Haan, K. H.; de Boer, J. L.; Teuben, J. H.; Spek, A. L.; Kojic-Prodic, B.; Hays, G. R.; Huis, R. *Organometallics* **1986**, *5*, 1726–1733.
(63) We can typically detect pressure surges from desolvation of THF-containing organosamarium complexes.[64]
(64) Evans, W. J.; Hughes, L. A.; Hanusa, T. P. *Organometallics* **1986**, *5*, 1285–1291.
(65) The complexes have similar solubility and decompose on chromatographic supports.

C_5Me_5 resonances of the organosamarium products of the pyridine reaction change after 15 min and continue to change for days. No single organometallic product has been isolated from this reaction so far.

Complex **2** reacts faster with H_2 than with hexane such that hydrogenolysis of the Sm–C bond in **2** can be achieved. $[(C_5Me_5)_2Sm(\mu\text{-}H)]_2$[30] precipitates from a hexane solution of **2** under H_2 and can be isolated in 85% yield (eq 6).

$$2(C_5Me_5)_2SmMe(THF) + 2H_2 \rightarrow [(C_5Me_5)_2Sm(\mu\text{-}H)]_2 + 2CH_4 \quad (6)$$

Complex **2** also reacts faster with ethylene than with solvent and functions as a polymerization catalyst. Complex **1** polymerizes ethylene as well. Hence, 0.008 M solutions of each consume 30 psi of ethylene in a 3-oz vessel within 15 min.

Discussion

Synthesis. $(C_5Me_5)_2Sm(THF)_2$ reduces Me_3Al to form a finely divided black precipitate (presumably aluminum metal) and the tetramethylaluminate $(C_5Me_5)_2Sm[(\mu\text{-}Me)AlMe_2(\mu\text{-}Me)]_2Sm(C_5Me_5)_2$ (**1**). The reaction may occur in the same way that alkali metals reduce AlR_3 to form AlR_4^- salts[36,40,66,67] (eq 7; M = alkali metal). Parallels between the reactivity of $(C_5Me_5)_2Sm(THF)_2$ and the alkali metals have been noted before.[3-5,31,68] The

$$3M + AlR_3 \rightarrow Al + 3RM \xrightarrow{3R_3Al} 3MAlR_4 + Al \quad (7)$$

$(C_5Me_5)_2Sm(THF)_2$ analogue of eq 7 is presented in eq 8. The

$$3Cp^5{}_2SmMe(THF)_2 + AlMe_3 \rightarrow Al + 3Cp^5{}_2SmMe(THF) \xrightarrow{3AlMe_3} 1.5Cp^5{}_2Sm[(\mu\text{-}Me)AlMe_2(\mu\text{-}Me)]_2SmCp^5{}_2 + Al \quad (8)$$

formation of metallic precipitate is consistent with the first part of this reaction pathway. The second part of eq 8, which is just the reverse of the equilibrium used to synthesize **2** (eq 3), has been independently verified, i.e., removal of solvent from a THF solution of $(C_5Me_5)_2SmMe(THF)$ and $AlMe_3$ gives **1**.[69]

In a related system, the unsolvated $(C_5Me_5)_2Sm$[5] reacts similarly with $AlEt_3$ to form $(C_5Me_5)_2Sm(\mu\text{-}Et)_2AlEt_2$ (**11**) and aluminum.[31] The $AlEt_3$ reaction gives a smaller yield than the $AlMe_3$, which is consistent with higher reactivity of the likely intermediate, $(C_5Me_5)_2SmEt$.

The formation of $(C_5Me_5)_2SmMe(THF)$ (**2**) by cleavage of $AlMe_3$ from the tetraalkylaluminate **1** (eq 3) has direct precedent in organoscandium chemistry (eq 9).[51] A similar cleavage of

$$(C_5H_5)_2Sc(\mu\text{-}Me)_2AlMe_2 + THF \rightarrow (C_5H_5)_2ScMe(THF) + AlMe_3 \quad (9)$$

lanthanide analogues with pyridine as the displacing base is also known (eq 10; Ln = Yb, Y).[51] This method has also been used to form $(C_5Me_5)_2YbMe(OEt_2)$ from $(C_5Me_5)_2Yb(\mu\text{-}Me)_2AlMe_2$ and Et_2O.[70,71]

$$2(C_5H_5)_2Ln(\mu\text{-}Me)_2AlMe_2 + 2C_5H_5N \rightarrow [(C_5H_5)_2Ln(\mu\text{-}Me)]_2 + 2AlMe_3(NC_5H_5) \quad (10)$$

Structure. The dimeric structure of **1** was surprising given the known crystal structure of monomeric $(C_5H_5)_2Yb(\mu\text{-}Me)_2AlMe_2$ (**12**)[39] and the monomeric formulas in the literature for $(C_5Me_5)_2Lu(\mu\text{-}Me)_2AlMe_2$ (**13**) and $(C_5Me_5)_2Yb(\mu\text{-}Me)_2AlMe_2$ (**14**).[14,55,70,71] However, the recent studies on the monomer dimer equilibria of $(C_5Me_5)_2Y(\mu\text{-}Me)_2AlMe_2$ (**15**)[48,49,53] and $(C_5Me_5)_2Lu(\mu\text{-}Me)_2AlMe_2$[48,49] together with the samarium results reported here indicate that monomer–dimer equilibria are the rule rather than the exception for $(C_5Me_5)_2LnAlMe_4$ complexes.

Indeed, one may ask why (or if) the $(C_5H_5)_2Ln(\mu\text{-}Me)_2AlMe_2$ complexes do not have an accessible dimeric form also. An obvious point of difference in these C_5H_5 systems is the size of the cyclopentadienyl rings and this may answer the above question. A $(\mu\text{-}Me)_2AlMe_2$ unit may be able to coordinate to a $(C_5H_5)_2Ln$ moiety without unfavorable steric interactions, whereas steric crowding may occur when it is coordinated to a $(C_5Me_5)_2Ln$ fragment.

It has already been noted for the $(C_5Me_5)_2Yb(\mu\text{-}X)_2Li(OEt_2)_2$ complexes (X = Cl, I) that steric crowding causes the C_5Me_5 rings to be eclipsed when the X ligand is large, i.e., in the iodide case.[72] Similarly, $(C_5Me_5)_2Yb(\mu\text{-}Cl)_2AlCl_2$ has (C_5Me_5 ring carbon)–(bridging chloride) contacts less than the sum of their van der Waals radii.[72] It is possible that the (C_5Me_5 ring carbon)–(methyl) contacts in monomeric $(C_5Me_5)_2Sm(\mu\text{-}Me)_2AlMe_2$ are greater than in dimeric **1**. Hence, when **1** crystallizes, the dimeric form is preferred.

Clearly, the dimeric form of **1** allows the $AlMe_4$ unit to be further from the metal center since the Sm–C(Me) average distance is 2.746 (1) Å compared to a Sm–C(CH_2) distance of 2.662 (4) Å in monomeric $(C_5Me_5)_2Sm(\mu\text{-}Et)_2AlEt_2$.[31] The dimeric form also allows more flexibility in the placement of the two carbon atoms attached to each Sm. A bidentate $(\mu\text{-}Me)_2AlMe_2$ ligand in a monomeric complex has a limited bite angle due to the constraints of the C–Al–C angle. In contrast, the two $(\mu\text{-}Me)AlMe_2(\mu\text{-}Me)$ ligands in the dimer can adopt a variety of C–Sm–C angles and C···C nonbonding distances. For example, the C(22)–C(21′) nonbonding distance between the two carbon atoms of two separate $AlMe_4$ groups attached to Sm(1) in **1**, 3.709 Å, is much larger than the typical C(21)–C(22) distance of 3.178 Å between two carbon atoms of the same $AlMe_4$ group.

$(C_5Me_5)_2Sm(\mu\text{-}Et)_2AlEt_2$ presumably has less propensity to form a dimeric structure analogous to that of **1** since the carbon atom in the Sm–C–Al bridge would be substituted with a methyl group. This methyl group would probably have unfavorable steric interactions with the C_5Me_5 rings in a dimeric structure. Note that in $(C_5Me_5)_2Sm(\mu\text{-}Et)_2AlEt_2$,[31] which has a C($\mu$-Et)–Sm–C($\mu$-Et) angle of 80.4 (4)°, the methyl group in the ethyl bridge is bent away from the C_5Me_5 rings such that the Sm–C–C angle is 170 (4)°. If the ethyl complex formed a dimer and maintained the 85.0 (5)° C(22)–Sm(1)–C(21′) angle in **1**, the methyl group of the ethyl bridge would be forced too close to the C_5Me_5 rings. If the methyl group moved away from the C_5Me_5 rings to reduce an unfavorable interaction, the bridging carbon atom could not adopt a trigonal-pyramidal conformation.

The nearly linear Sm–C–Al angles in **1** may occur because this is the best compromise structure given the steric constraints present in the molecule. If these angles were more acute and if the eight-membered $Sm_2Al_2C_4$ ring were still maintained, the C–Sm–C angles would have to be much larger than the 85.0 (5)° in **1**. For example, rough calculations maintaining the current bond lengths and C–Al–C angles indicate that to lower the C–Al–Sm angle to only 160°, a C–Sm–C angle of 120° would be necessary. The latter angle would cause strongly repulsive C(C_5Me_5)–C(μ-Me) contacts and would not be readily accommodated in a bent metallocene.

In summary, molecules such as $(C_5H_5)_2Ln(\mu\text{-}Me)_2AlMe_2$ may have no steric reason to form the dimeric structures found in the $(C_5Me_5)_2Ln[(\mu\text{-}Me)AlMe_2(\mu\text{-}Me)]_2Ln(C_5Me_5)_2$ molecules. For the pentamethylcyclopentadienyl species $[(C_5Me_5)_2Ln(\mu\text{-}Me)_2AlMe_2]_n$, both monomeric and dimeric forms are accessible, but the dimers are preferred sterically. For $(C_5Me_5)_2Ln(\mu\text{-}Z)_2AlZ_2$ complexes where Z = Cl the longer Ln–(μ-Z) bond

(66) Mole, T.; Jeffery, E. A. *Organoaluminum Compounds*; Elsevier: Amsterdam, 1972; p 178 and references therein.
(67) Zakharkin, L. I.; Gavrilenko, V. V. *J. Gen. Chem. USSR Engl. Transl.* **1962**, *32*, 688–690.
(68) Evans, W. J.; Ulibarri, T. A. *J. Am. Chem. Soc.* **1987**, *109*, 4292–4297.
(69) Note, however, that $(C_5Me_5)_2YbMe_2Li(OEt_2)_2$, which reacts with 1 equiv of $AlMe_3$ to form $(C_5Me_5)_2YbMe(THF)$, reportedly fails to react with excess $AlMe_3$ to form $(C_5Me_5)_2YbMe_2AlMe_2$.[70]
(70) Watson, P. L. *J. Chem. Soc., Chem. Commun.* **1980**, 652–653.
(71) Watson, P. L. *J. Am. Chem. Soc.* **1982**, *104*, 337–339.
(72) Watson, P. L.; Whitney, J. F.; Harlow, R. L. *Inorg. Chem.* **1981**, *20*, 3271–3278.

reduces the steric tendency to form dimers and for Z = Et the substitution on the bridging carbon disfavors the dimeric form. This variation in structure based on small differences is not unusual for molecules of this type as shown by the numerous ways in which "$(C_5Me_5)_2SmCl$" can crystallize.[34,56]

In contrast to the unexpected structure of **1**, the structure of $(C_5Me_5)_2SmMe(THF)$ has numerous structural analogues.[28,29,56,57] A potentially unusual feature about the structure of **2** is the possibility that agostic Sm–H interactions exist as postulated for $(C_5Me_5)_2YMe(THF)$.[53,57] Unfortunately, neither the structure nor the spectral properties of **2** provide definitive evidence for such an interaction.

Reactivity. $(C_5Me_5)_2SmMe(THF)$ displays several reactivity patterns typical of a lanthanide alkyl complex.[4,14,60,73-75] Hence, it reacts with hydrogen via hydrogenolysis to make a hydride complex,[30,42,76,77] its reactivity is inhibited by THF,[4,42] and it polymerizes ethylene.[14,55,71,78]

On the basis of the high metalation reactivity reported for $(C_5Me_5)_2LuZ \rightleftharpoons (C_5Me_5)_2ZLu(\mu\text{-}Z)Lu(C_5Me_5)_2$ (Z = Me, H)[14,15,79] and the extensive study of "σ-bond metathesis" by $(C_5Me_5)_2ScZ$ complexes,[16] one would expect monomeric *unsolvated* $(C_5Me_5)_2SmMe$ to react readily with a variety of CH bonds. On the other hand, on the basis of the samarium structures of $[(C_5Me_5)_2Sm(\mu\text{-}Cl)]_3$[33] and $[(C_5Me_5)_2Sm(\mu\text{-}H)]_2$,[30] $(C_5Me_5)_2SmMe$ might well exist as an oligomer with less reactivity toward CH activation if it had bridging rather than terminal methyl groups. This is the case with $[(C_5Me_5)_2Sm(\mu\text{-}H)]_2$[80] and there are many examples in trivalent lanthanide chemistry which show that bridging ligands are less reactive than terminal ligands.[4,42,60] $(C_5Me_5)_2SmMe(THF)$ did not appear to lose THF of solvation upon heating under vacuum but instead decomposed. If $(C_5Me_5)_2SmMe$ did form, it apparently was too reactive to isolate.

We found, however, that the *solvated* $(C_5Me_5)_2SmMe(THF)$ has high CH activation reactivity. This is a marked difference from the $(C_5Me_5)_2LnMe(THF)$ complexes (Ln = Lu,[55] Yb,[55] Y[57]) for which no comparable reactivity has been reported. In the scandium system,[16] THF of solvation also reduces reactivity. Hence, $(C_5Me_5)_2ScCl(THF)$ fails to react with alkyllithium reagents and $(C_5Me_5)_2ScH(THF)$ is much less reactive than $(C_5Me_5)_2ScH$. The fact that $(C_5Me_5)_2SmMe(THF)$ is so much more reactive than the Sc, Y, and Lu analogues can be explained by the larger size of the metal. The samarium complex is sterically less saturated and hence more reactive.[4,60]

Considering the variations in reactivity found for the $(C_5Me_5)_2MZ$ complexes (M = Sc, Y, Lu; Z = Me, H) due to their differences in steric factors, charge to radius ratios, and M–C and M–H bond strengths,[15,16,79] one expects that $(C_5Me_5)_2SmMe(THF)$ will display its own characteristic variations in CH reactivity. Indeed, our preliminary survey of the reactivity of **2** shows this to be the case.

In particular, $(C_5Me_5)_2SmMe(THF)$ is much more reactive with alkane solvents than $(C_5Me_5)_2ScMe$ (**16**) or $[(C_5Me_5)_2LuMe]_{1,2}$ (**17**). Whereas **16** reacts with cyclohexane at 80 °C over several days[16] and the reaction of **17** with CH_4 is studied in cyclohexane at 70 °C,[15] **2** reacts with cyclohexane at room temperature to form methane and a variety of products. **2** also reacts at room temperature with hexane and cyclooctane again giving complex mixtures. Note that cyclooctane traditionally has been found to be most unreactive to C–H activating complexes[11] and was used as an internal standard to study the reactions of **16** and **17** with methane at 70 °C. The high reactivity of **2** with hydrocarbons complicates a detailed analysis of its reactivity since none of the common solvents are inert.

We have done a preliminary kinetic study of the reaction of **2** with C_6D_6 under pseudo-first-order conditions in C_6D_6 which goes cleanly in high yield. The 1.8×10^{-2} s^{-1} rate of reaction at 75 °C can be compared to a k_2 of 4.7 (1) $\times 10^{-6}$ s^{-1} M^{-1} for the reaction of $[C_5(CD_3)_5]_2ScMe$ (**18**) with excess C_6D_6 in C_6D_{12}[16] and a k_1 of 0.2×10^{-4} s^{-1} and a k_2 of 1×10^{-4} M^{-1} s^{-1} for the reaction of **17** with C_6D_6 at 70 °C[15] where k_1 and k_2 are defined in eq 11 and 12. The activation parameters for the $\mathbf{2}/C_6D_6$

$$(C_5Me_5)_2MMe \xrightarrow[-CH_4]{k_1} [(C_5Me_5)M(C_5Me_4CH_2)]_n \xrightarrow{C_6D_6} (C_5Me_5)(C_5Me_4CH_2D)MC_6D_5 \quad (11)$$

$$(C_5Me_5)_2MMe + C_6D_6 \xrightarrow{k_2} (C_5Me_5)_2MC_6D_5 + CH_3D \quad (12)$$

reaction, $\Delta H^{\ddagger} = 16.5 \pm 0.6$ kcal mol^{-1} and $\Delta S^{\ddagger} = -19 \pm 4$ eu, determined over the temperature range 55–85 °C, are similar to those found for the $\mathbf{18}/C_6H_6$ reaction,[16] $\Delta H^{\ddagger} = 18.9$ (2) kcal mol^{-1} and $\Delta S^{\ddagger} = -23$ (2) eu, determined at 42–67 °C. These data suggest that C–H bond activation by the samarium system may be mechanistically similar to that of the scandium system.

In both the Sc and Lu systems, evidence exists for two competing pathways for C–H activation: a unimolecular (eq 11, M = Sc, Lu) and a bimolecular route (eq 12). The relative importance of these routes can be measured by the amount of CH_4 formed compared to CH_3D or by the ratio of k_1/k_2. For Sc, the CH_4:CH_3D ratio is temperature dependent and varies from 1:3 at 60 °C to 1:1 at 125 °C.[16] For Lu, k_1/k_2 is 0.2 at 70 °C.[15] In contrast, the Sm system forms CH_4 exclusively in its reaction with C_6D_6 (eq 4). This suggests that the intramolecular decomposition of **2** is faster than a bimolecular metalation reaction and that the decomposition product reacts very quickly. Since **2** does not react with benzene in THF, we presume THF dissociation is the first step in the reaction. These postulates are summarized in eq 13–16 ($Cp^5 = C_5Me_5$) and in the sequence $k_3 > k_1 \gg k_2$. The facile formation of the undetected "$[Cp^5Sm(C_5Me_4CH_2)]_n$" is not in-

$$Cp^5_2SmMe(THF) \rightleftharpoons Cp^5_2SmMe + THF \quad (13)$$

$$Cp^5_2SmMe \xrightarrow{k_1} "[Cp^5Sm(C_5Me_4CH_2)]_n" + CH_4 \quad (14)$$

$$Cp^5_2SmMe + C_6D_6 \xrightarrow{k_2} Cp^5_2Sm(C_6D_5) + CH_3D \quad (15)$$

$$"[Cp^5Sm(C_5Me_4CH_2)]_n" + C_6D_6 \xrightarrow{k_3} Cp^5(C_5Me_4CH_2D)Sm(C_6D_5) \quad (16)$$

consistent with the possibility that $(C_5Me_5)_2LnMe(THF)$ complexes have agostic Ln–H interactions as postulated for the Ln = Y complex.[57] Prior interaction of a methyl hydrogen atom with the metal in either $(C_5Me_5)_2SmMe(THF)$ or $(C_5Me_5)_2SmMe$ could facilitate the CH_4 extrusion. This undetected intermediate could have a variety of structures including a monomeric intrametalated "tuck-in" form[14,16,81-83] $(C_5Me_5)Sm(C_5Me_4CH_2)$, a dimeric form $(C_5Me_5)Sm(\mu\text{-}C_5Me_4CH_2)_2Sm(C_5Me_5)$,[84] or a hydride form $(C_5Me_5)Sm(\mu\text{-}C_5Me_4CH_2)(\mu\text{-}H)Sm(C_5Me_5)_2$,

(73) Marks, T. J.; Ernst, R. D. In *Comprehensive Organometallic Chemistry*; Wilkinson, G., Stone, F. G. A., Abel, E. W., Eds.; Pergamon: New York, 1982; Chapter 21.
(74) Schumann, H.; Genthe, W. In *Handbook on the Physics and Chemistry of Rare Earths*; Gschneidner, K. A., Jr., Eyring, L., Eds.; Elsevier: Amsterdam, 1985; Vol. 7, Chapter 53 and references therein.
(75) Forsberg, J. H.; Moeller, T. In *Gmelin Handbook of Inorganic Chemistry*, 8th ed.; Moeller, T., Kruerke, U., Schleitzer-Rust, E., Eds.; Springer-Verlag: Berlin, 1983; Part D6, pp 137–282.
(76) Jeske, G.; Lauke, H.; Mauermann, H.; Swepston, P. N.; Schumann, H.; Marks, T. J. *J. Am. Chem. Soc.* **1985**, *107*, 8091–8103 and references therein.
(77) den Haan, K. H.; Teuben, J. H. *Recl. Trav. Chim. Pays-Bas* **1984**, *103*, 333–334.
(78) Ballard, D. G. H.; Courtis, A.; Holton, J.; McMeeking, J.; Pearce, R. *J. Chem. Soc., Chem. Commun.* **1978**, 994–995.
(79) Watson, P. L. *J. Chem. Soc., Chem. Commun.* **1983**, 276–277.
(80) Evans, W. J.; Grate, J. W.; Ulibarri, T. A., unpublished results.
(81) Bercaw, J. E. *J. Am. Chem. Soc.* **1974**, *96*, 5087–5095.
(82) Cloke, F. G. N.; Green, J. C.; Green, M. L. H.; Morley, C. P. *J. Chem. Soc., Chem. Commun.* **1985**, 945–946.
(83) Cf.: Pattiasina, J. W.; Hissink, C. E.; de Boer, J. L.; Meetsma, A.; Teuben, J. H.; Spek, A. L. *J. Am. Chem. Soc.* **1985**, *107*, 7758–7759.
(84) Thompson, M. E.; Bercaw, J. E. *Pure Appl. Chem.* **1984**, *56*, 1–11.

analogous to that proposed for an yttrium complex.[85]

The reaction of **2** with toluene also has a parallel in the Sc system.[16] The reaction of **16** with toluene at 80 °C gives $(C_5Me_5)_2ScCH_2C_6H_5$ as the kinetic product which reacts further to form a mixture of tolyl isomers. At room temperature **2** forms the benzyl product exclusively from toluene.

It is more difficult to compare the reactivity of **2** with pyridine and Et_2O to that of **16** and **17** with these substrates. Both the Sc and Lu complexes react with pyridine to form the metalated species $(C_5Me_5)_2M(\eta^2\text{-}C_5H_4N)$ and methane. NMR evidence for a pyridine adduct intermediate, $(C_5Me_5)_2MMe(NC_5H_5)$, is observed.[16,79] In the Sc case, the reaction was run in refluxing benzene. For the samarium complex **2**, pyridine metalation is rapid at room temperature and a mixture of other products is formed which evolves over a several day period.

The reaction of **2** with Et_2O to form the ethoxide complex $(C_5Me_5)_2Sm(OEt)(THF)$ parallels the reaction of $[(C_5Me_5)_2LuH]$[14,15] with Et_2O to form $(C_5Me_5)_2LuOEt$.[79] However, no such reactivity has been reported for $(C_5Me_5)_2MMe(OEt_2)$ complexes (M = Lu, Yb)[55,71] and $(C_5Me_5)_2YbMe(OEt_2)$ was stable enough to allow an X-ray crystal structure determination.[86]

Conclusion

The reaction of $(C_5Me_5)_2Sm(THF)_2$ with Me_3Al has provided two reactive samarium methyl complexes, **1** and **2**. This preliminary survey of the reactivity of **1** and **2** shows that an extensive organometallic chemistry will be available via these species. The initial studies of the C-H activation reactivity of **2** show parallels with unsolvated scandium and lutetium complexes and suggest that this is another complex capable of σ-bond metathesis with a variety of substrates. **2** appears to have some special characteristics in this regard which will form the basis for future investigations. Especially noteworthy is the high reactivity with alkane substrates. With the extension of the C-H metalation reactivity from the small metals Sc, Y, and Lu to the midsized Sm, it appears that this type of reactivity will be general for the lanthanides and similar metals if the proper ligand set and coordination environment are provided.

Acknowledgment. We thank the National Science Foundation for support of this research, the University of California for a Presidential Postdoctoral Fellowship (to L.R.C.), Donald K. Drummond for collecting and partially solving an X-ray data set, Professor Frank J. Feher for helpful discussions, and Dr. Matthew B. Zielinski for arranging the molecular weight distribution measurements. Funds for the purchase of the X-ray equipment were made available from NSF Grant CHE-85-14495.

Registry No. 1a, 115756-72-4; **1b**, 115756-73-5; **2**, 115731-48-1; $AlMe_3$, 75-24-1; $(C_5Me_5)_2Sm(THF)_2$, 79372-14-8; $C_6D_5CD_3$, 2037-26-5; Et_2O, 60-29-7; C_6D_6, 1076-43-3; $(C_5Me_5)_2Sm(OEt)(THF)$, 115731-49-2; $(C_5Me_5)_2Sm(C_6D_5)(THF)$, 115731-50-5; $(C_5Me_5)_2Sm(CH_2C_6H_5)(THF)$, 115731-51-6; $(C_5Me_5)_2Sm(CD_2C_6D_5)(THF)$, 115731-52-7; C_6D_{12}, 1735-17-7; $[(C_5Me_5)_2Sm(\mu\text{-}H)]_2$, 84751-30-4; H_2, 1333-74-0; toluene, 108-88-3; pyridine-d_5, 7291-22-7; cyclooctane, 292-64-8; ethylene, 74-85-1; polyethylene, 9002-88-4.

Supplementary Material Available: Tables of complete bond distances and angles and thermal parameters (5 pages); listings of observed and calculated structure factor amplitudes (20 pages). Ordering information is given on any current masthead page.

(85) den Haan, K. H.; Teuben, J. H. *J. Chem. Soc., Chem. Commun.* **1986**, 682-683.
(86) Unpublished results cited in ref 55.

Stereochemistry of Vinylallene Cycloadditions

Hans J. Reich,* Eric K. Eisenhart, Wesley L. Whipple, and Martha J. Kelly

Contribution from the Department of Chemistry, University of Wisconsin, Madison, Wisconsin 53706. *Received February 1, 1988*

Abstract: Diels-Alder cycloadditions of three vinylallenes 1,2,4-octatriene (**6**), 2,3,5-nonatriene (**7**), and 2-methyl-2,3,5-nonatriene (**8**) with maleic anhydride and dimethyl fumarate were studied. Product ratios were dominated by the steric and electronic effects between the out-of-plane substituents on the vinylallene terminus and substituents on the dienophile. Excellent control of exocyclic double-bond stereochemistry can be achieved. The cycloaddition of methylmaleic anhydride with **8** gave only a single regio- and stereoisomer, compound **26**, the product formed by approach of vinylallene and dienophile in the least hindered orientation. Configurational assignments to the six isomeric diesters [(*E*)-**16**, (*Z*)-**16**, (*E*)-**17**, (*E*)-**18**, (*Z*)-**18**, (*E*)-**19**] formed by reaction of **7** with maleic anhydride and dimethyl maleate were made on the basis of detailed conformational analysis using MM2 and consideration of proton and carbon NMR spectroscopic data, NOE studies, and 2D proton-carbon correlations. Rate studies of the reaction of a series of vinylallenes with *N*-methylmaleimide also supported the concept that steric interactions with allene substituents play an important role in the transition state. Vinylallenes are slightly more reactive than comparably substituted 1,3-butadienes.

The cycloaddition reactions of vinylallenes have the potential for regio- and stereochemical control resulting from the interaction between the out-of-plane substituents at the terminus of the allene and the dienophile. These effects have not been well defined; in fact, Diels-Alder cycloadditions of vinylallenes and bis(allenes) have in general been little studied.[1a,b,2-4] We report here our work on some aspects of this topic using reactions of several allenes with maleate and fumarate dienophiles.

Previous work on vinylallene Diels-Alder cycloadditions has shown that their reactivity is comparable to similarly substituted

(1) (a) Reich, H. J.; Eisenhart, E. K. *J. Org. Chem.* **1984**, *49*, 5282. (b) Reich, H. J.; Eisenhart, E. K.; Olson, R. E.; Kelly, M. J. *J. Am. Chem. Soc.* **1986**, *108*, 7791. (c) Reich, H. J.; Kelly, M. J.; Olson, R. E.; Holtan, R. C. *Tetrahedron* **1983**, *39*, 949. (d) Reich, H. J.; Wollowitz, S. *J. Am. Chem. Soc.* **1982**, *104*, 7051. (e) Reich, H. J.; Renga, J. M.; Reich, I. L. *J. Am. Chem. Soc.* **1975**, *97*, 5434.
(2) (a) Bertrand, M.; Grimaldi, J.; Waegell, B. *Bull. Soc. Chim. Fr.* **1971**, 962. (b) Yoshida, K.; Grieco, P. A. *Chem. Lett.* **1985**, 155. (c) Jones, E. R. H.; Lee, H. H.; Whiting, M. C. *J. Chem. Soc.* **1960**, 341. Heldeweg, R. F.; Hogeveen, H. *J. Org. Chem.* **1978**, *43*, 1916.
(3) Santelli, M.; Abed, D. E.; Jellal, A. *J. Org. Chem.* **1986**, *51*, 1199. Fedorova, A. V.; Petrov, A. A. *J. Gen. Chem. USSR* **1962**, (*Engl. Trans.*) *32*, 3471. Angelov, C. M.; Mondeshka, D. M.; Tancheva, T. N. *J. Chem. Soc., Chem. Commun.* **1985**, 647. Mödlhammer, U.; Hopf, H. *Angew. Chem., Int. Ed. Engl.* **1975**, *14*, 501. Fedorova, A. V.; Petrov, A. A. *Zh. Obshch. Khim.* **1962**, *32*, 3537. Dangyan, Y. M.; Voskanyan, M. G.; Zurabyan, N. Z.; Badanyan, S. O. *Arm. Khim. Zh.* **1979**, *32*, 460; *Chem. Abstr.* **1980**, *92*, 76604.
(4) Intramolecular: Snider, B. B.; Burbaum, B. W. *J. Org. Chem.* **1983**, *48*, 4370. Deutsch, E. A.; Snider, B. B. *J. Org. Chem.* **1982**, *47*, 2682. Bartlett, A. J.; Laird, T.; Ollis, W. D. *J. Chem. Soc., Chem. Commun.* **1974**, 496.

0002-7863/88/1510-6432$01.50/0